Materials Today Bio 16 (2022) 100406

Contents lists available at ScienceDirect

Materials Today Bio

journal homepage: www.journals.elsevier.com/materials-today-bio

Developmentally engineered bio-assemblies releasing neurotrophic exosomes guide in situ neuroplasticity following spinal cord injury

Jin Yan [a,1], Liqiang Zhang [b,1], Liya Li [b], Wangxiao He [b,c,*], Wenjia Liu [a,b,**]

[a] National & Local Joint Engineering Research Center of Biodiagnosis and Biotherapy, The Second Affiliated Hospital of Xi'an Jiaotong University, Xi'an 710004, China
[b] Institute for Stem Cell & Regenerative Medicine, The Second Affiliated Hospital of Xi'an Jiaotong University, Xi'an 710004, China
[c] Department of Medical Oncology and Department of Talent Highland, The First Affiliated Hospital of Xi'an Jiaotong University, Xi'an 710061, China

ARTICLE INFO

Keywords:
Bio-assemblies
Exosome
Developmentally engineered
Neuroplasticity
Spinal cord injury

ABSTRACT

The emerging tissue-engineered bio-assemblies are revolutionizing the regenerative medicine, and provide a potential program to guarantee predictive performance of stem-cell-derived treatments *in vivo* and hence support their clinical translation. Mesenchymal stem cell (MSC) showed the attractive potential for the therapy of nervous system injuries, especially spinal cord injury (SCI), and yet failed to make an impact on clinical outcomes. Herein, under the guidance of the embryonic development theory that appropriate cellular coarctations or clustering are pivotal initiators for the formation of geometric and functional tissue structures, a developmentally engineered strategy was established to assemble DPMSCs into a bio-assembly termed Spinor through a three-level sequential induction programme including reductant, energy and mechanical force stimulation. Spinor exhibited similar geometric construction with spinal cord tissue and attain autonomy to released exosome with the optimized quantity and quality for suppressing cicatrization and inflammation and promoting axonal regeneration. As a spinal cord fascia and exosome mothership, Spinor guided the *in-situ* neuroplasticity of spinal cord *in vivo*, and caused the significant motor improvement, sensory recovery, and faster urinary reflex restoration in rats following SCI, while maintaining a highly favorable biosafety profile. Collectively, Spinor not only is a potentially clinical therapeutic paradigm as a living "exosome mothership" for revisiting Prometheus' Myth in SCI, but can be viewed allowing developmentally engineered manufacturing of biomimetic bio-assemblies with complex topology features and inbuilt biofunction attributes towards the regeneration of complex tissues including nervous system.

1. Introduction

In recent years, the emerging tissue-engineered advanced therapy medicinal products (TE-ATMPs), particularly tissue-engineered bio-assemblies, are revolutionizing the regenerative medicine, and provide a potential program to guarantee predictive performance of stem-cell-derived treatments *in vivo* and hence support their clinical translation [1,2]. Although some successes have been achieved in development of TE-ATMPs, such as tissue-engineered bladder, skin, cartilage, trachea and blood vessels, towards replacing damaged organs or restoring their function, an enormous challenge remain regarding to the rational construction of TE-ATMPs with robustness and predictive outcomes [3]. To address it, a "developmental engineering" strategy conceptual and technical merging of developmental biology and biological engineering is arising, which strive to mimic developmental events such as cellular self-assembly and condensation to guarantee the predictive function and robustness of the constructed TE-ATMPs [1,4]. By this way, appropriate cellular self-assemblies are pivotal initiators for the formation of geometric and functional tissue structures that capable of executing developmental programs to advocate and facilitate the organogenesis processes including the auto-proliferative differentiation and extracellular vesicles (exosome) release [5,6]. Therefore, it can be anticipated that developmentally engineered bio-assemblies can tackle the hurdle of the limited predictive *in vivo* performance of tissue-engineered medicinal products in the repair of complex tissues such as nervous system.

Spinal cord injury (SCI), one of the toughest central nervous system

* Corresponding author. Institute for Stem Cell & Regenerative Medicine, The Second Affiliated Hospital of Xi'an Jiaotong University, Xi'an 710004, China.
** Corresponding author. National & Local Joint Engineering Research Center of Biodiagnosis and Biotherapy, The Second Affiliated Hospital of Xi'an Jiaotong University, Xi'an 710004, China.
E-mail addresses: hewangxiao5366@xjtu.edu.cn (W. He), wenjialiu@xjtu.edu.cn (W. Liu).
[1] These authors contributed equally.

https://doi.org/10.1016/j.mtbio.2022.100406
Received 30 May 2022; Received in revised form 12 August 2022; Accepted 18 August 2022
Available online xxxx

injuries to treat, occurs with a worldwide incidence of over one ten-thousandth annually [7,8]. Cruelly, patients suffering from this complicated neuropathological condition have to endure not only the physical functional dysfunction and even paralysis but also the heavy mental burden to their individuals as well as their families [9,10]. To bail out this dilemma and promote functional recovery of spinal cord, two general strategies have emerged: 1) surgical operation in conjunction with intravenous high-dose neuritepromoting factors such as antagonists to extracellular inhibitory molecule, neurotrophic factors, neuroprotective factors and permissive substrates [11–13], and 2) stem cell and/or TE-ATMPs transplantation towards replacing the nerve defect and promoting the axon regeneration [9,14]. Over the past decade, the first therapeutic strategy resulted in over 35% drop in SCI deaths, because that the popularity of the surgical decompression as well as connection

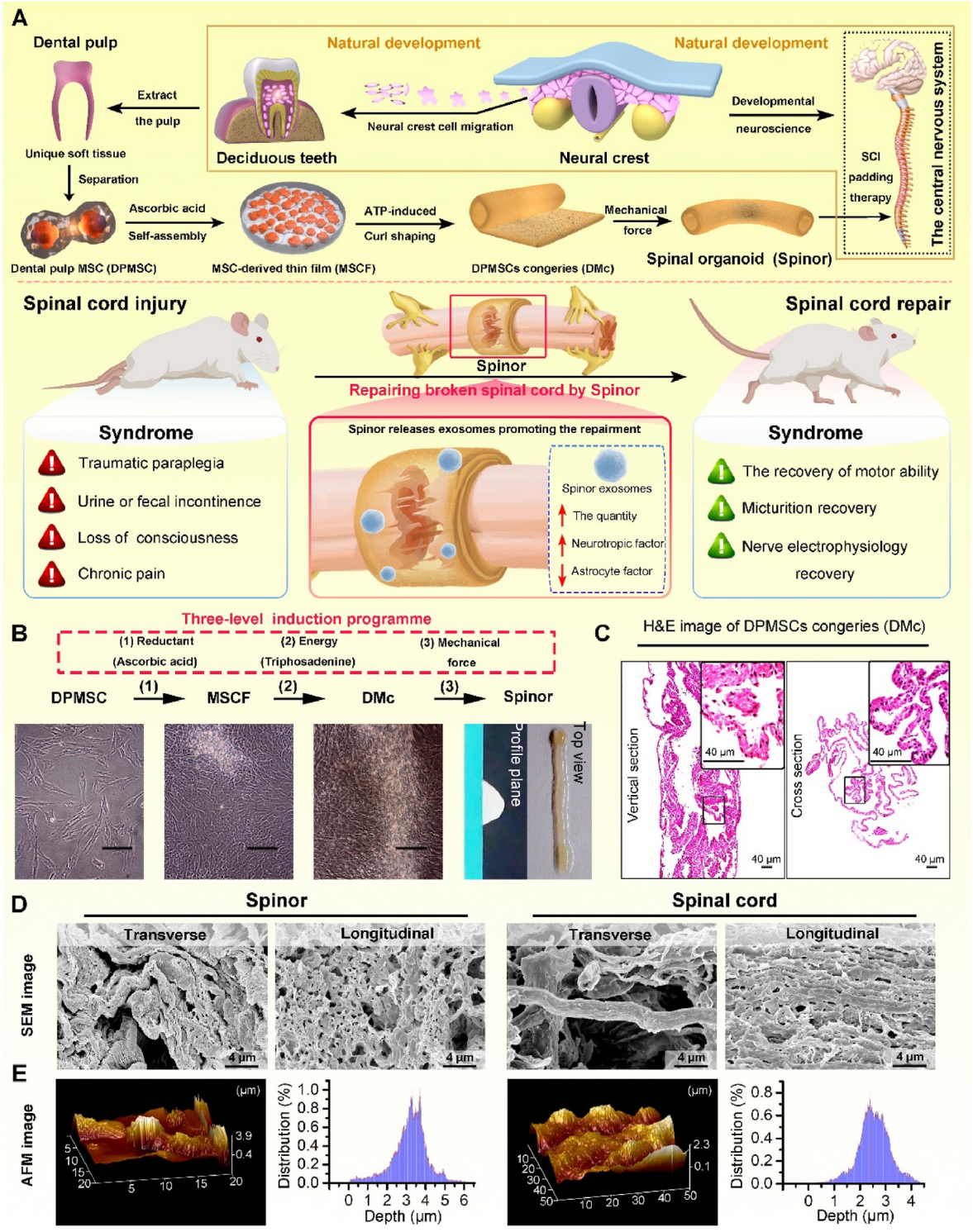

Fig. 1. The design and characterization analysis of the developmentally engineered bio-assembly termed Spinor. (A) Schematic depiction for construction of Spinor and its biofunction. (B) Schematic depiction and photos for construction of Spinor. (C) The representative images of H&E-stained DPMSCs congeries (DMc) sections. (D&E) Scanning electron microscope (SEM, D) and atomic force microscope (AFM, E) images of Spinor and spinal cord sections.

technique in SCI healing treatment and the development of the adjuvant medical therapy promote the neuroplasticity derived from axonal sprouting and synaptic remodeling. [8, 14] However, this therapeutic strategy has so far failed to make an impact on the course of the SCI and on clinical outcomes in reversing the physical functional dysfunction and even paralysis of patients [8,9,15]. As for the second strategy, by the way of the stem cell and/or TE-ATMPs transplantation, some positive clinical progresses have been achieved [7,16–22], in especial of chronic SCI therapy [23], whereas significant challenges remain with regard to robust regeneration of injured axons and substantial functional recovery from severe or even complete SCI. Indeed, only a small amount of transplanted stem cells extremely fortunate to survive and a tiny part of them actually differentiate into neural cells in injured spinal cord [24,25]. Recently, accumulating evidence revealed that therapeutic efficacy recognized to stem cells attributed to the auxo-action of neuroplasticity profiting from their extracellular secretion in especial of extracellular microvesicles rather than cell replacement [10,26,27].

After SCI, to cope with the demands of neuronal activity and connective neurofeedback, neuroplasticity can occur whereby the transected axons spontaneously regrow across a lesion site in various forms encompassing collateral axonal sprouting as well as structural synaptic remodeling [28]. Theoretically, in this case, the fractured neural circuit can be reorganized, and the physiological function can be restored as a consequence [9]. Nevertheless, few axons actually regenerate successfully, especially for long distances, due to the troublesome physical and molecular barrier - Astrocyte scar [28]. After SCI, as limitans border between the lesion core and adjacent viable nerve, narrow astrocyte scars can restrict the spread of inflammation but block axon growth, invalidating the neuroplasticity [29,30]. Fortunately, neural stem cells (NSC)-and/or mesenchymal stem cell (MSC)-derived exosomes, a class of natural extracellular microvesicle of endosomal origin with grain diameter range from 50 to 150 nm, have been identified the strong biological function for promoting axons growth and suppressing astrocyte scars as well as inflammation [31–35]. As MSC is easy to obtain from funicle, endodontium, fat and et al. in sharp contrast to the intricate and destructive separation and extraction of NSC, increasing researches have revealed the potential of MSC and MSC-derived exosomes in SCI therapy [36,37]. Nevertheless, two high hurdles remain to overcome: 1) there exists limited knowledge about which kind of MSC exosomes is the best choice for SCI repair, and 2) exosomes therapeutics entails the use of time-consuming and laborious extraction process. Presumably because of these two hurdles, none of exosomes or their derivatives has so far been approved for clinical application towards promoting neuroplasticity.

During the embryonic development, neural plate invaginates to form the neural tube and the subsequent spinal cord [38], which was facilitated by the extracellular microvesicle derived from pluripotent cell at the margin of the neural plate (Fig. 1A) [39]. Herein, we firstly approved the optimal auxo-action in axons regeneration of exosome derived from pulp-derived MSC (DPMSC) that developed from these pluripotent cells at the margin of the neural plate (Fig. 1A). Next, Under the guidance of the embryonic development theory that appropriate cellular coarctations or aggregations are pivotal initiators for the formation of geometric and functional tissue structures [5,6], a developmentally engineered strategy was established to assemble DPMSCs into a bio-assembly through a three-level sequential induction programme including reductant, energy and mechanical force stimulation (Fig. 1A). Excitingly, in possession of the similar geometric construction and mechanical property with spinal cord, this bio-assembly is employed as a biomimetic **spin**al rest**or**er, thereby terming **Spinor**. More importantly, the Spinor-derived exosome showed its predictive *in vivo* performance in facilitating axonal sprouting and synaptic remodeling through releasing exosomes with the optimal quantity and auxo-action for promoting axons growth and suppressing astrocyte scars as well as inflammation (Fig. 1A). As a spinal cord fascia and exosome mothership, Spinor supported the reemergence of electrophysiological activity as well as behavior in rats with complete spinal cord injury and enabled them walking functional recovery. Collectively, Spinor will provide a promising clinical therapeutic application for severe or even complete SCI, and supported a new thought to amplify the intrinsic capabilities of stem-cells-derived exosome. More importantly, the developmentally engineered strategy established here will likely have a broad impact on the development of tissue-engineered advanced therapy medicinal products and reinvigorate the efforts for employing stem cells as well as their ramifications in the repair of complex tissues including nervous system.

2. Results and discussion

2.1. The exosome from DPMSC is more conducive to nerve regeneration than other MSC-derived exosomes

To explore the effect of MSC types on the exosome-acceerative nerve regeneration, three kinds of highly accessible MSCs respectively from dental pulp, umbilical cord and bone marrow were tested. Firstly, dental pulp-derived MSC (DPMSC), umbilical cord-derived MSC (UCMSC) and bone marrow-derived MSC (BMMSC) were identified by the paralleled expression of the MSC markers CD73, CD146 and CD105 and the concomitant absence of other cell-type markers CD11b, CD34 and CD45 (Fig. S1A). Next, four important neurotrophic factors were semi-quantified at transcriptional level by RT-PCR in the three MSCs, and it can be found in Fig. S1B that the relative expression of BDNF, b-FGF, CTNF and NT-3 were significantly greater in DPMSC than BMMSC and UCMSC. This result compelled us further investigated the action of exosomes from DPMSC. Towards this end, exosomes were extracted from DPMSC, BMMSC and UCMSC by isodensity centrifugation immediately following by size exclusion chromatography. Co-incubating with neuronal cells, DPMSC-derived exosomes showed the strongest effect on promoting the axonal sprouting in contrast to UCMSC-derived exosomes and BMMSC-derived exosomes (Fig. S1C&D). As shown in Fig. S1E, DPMSC exosome statistically significantly increased the branch points and neurite counts of neurons comparting with UCMSC and BMMSC exosome. Meanwhile, DPMSC-derived exosomes facilitate the elongation of the neuron length (Fig. S1E), further suggesting the auxo-action of DPMSC exosome in promoting the regeneration and differentiation of neurons.

2.2. Establishing developmentally engineered strategy to assemble DPMSCs into a bio-assembly

Firstly, the pluripotent stem cell characterization of DPMSCs were identified through their capacity of single-colony clusters formation (Fig. S2A) and osteogenic differentiation (Fig. S2B). Next, these DPMSC cultured with medium containing 10% FBS, increasing in number about 100-fold after 3 passages. Following these preparatory work, under the guidance of the embryonic development theory that appropriate cellular coarctations or clustering are pivotal initiators for the formation of geometric and functional tissue structures [5,6], a three-step developmentally engineered strategy was performed to assemble DPMSCs into a bio-assembly: step 1) simulating germ cell clustering and developing to induce DPMSCs assembly into MSC-derived thin file (MSCF) by the ascorbic acid (AA) stimulation, 2) simulating tissue development to induce MSCF coarctation into DPMSCs congeries (DM_C) *via* the triphosadenine (ATP) stimulation, and 3) simulating organogenesis to induce DMc crispation to Spinor through mechanical force (Fig. 1A and B). In details, AA was added into the medium to stimulate the self-assembly of DPMSC into a thin-film structure in this first step (Fig. 1A&B), because of the auxo-action of AA in the intercellular adhesion *via* collagenous fiber formation [40,41]. Moreover, to optimize the formation of MSCF, various concentrations of AA was applied, and it can be found that about 100 μg/ml AA had the strongest effects on the film construction (Fig. S3A) and collagen secretion (Fig. S3B). Moreover, AA at the dosage of 100 μg/ml induced the most collagen accumulation after 5-days incubation (Fig. S3C). After that in the second step, ATP was added into the culture

medium of MSCF to induce the formation of stacked arrangement [42] termed DMc, as evidenced by the photo and H&E staining in Fig. 1B and C. In the step 3, upon stripping off from dish and the following curling, DMc can be handily translated into bioactive spinor (Fig. 1A&B) to fill in the blanks after SCI and/or dress the wound of spinal cord. As evidenced by the scanning electron microscope (SEM) images (Fig. 1D), Spinor possessed well-interconnected pore internal structure that is analogous to the internal anatomical structure of spinal cord, which were desired to support neural stem cells attachment, proliferation, differentiation and migration, thereby guiding and promoting the axon regeneration [43–45]. Furthermore, atomic force microscope (AFM) measurement in Fig. 1E revealed that the longitudinal section of Spinor had the similar surface topography and mechanical property with the spinal cord, suggesting the splendid biological and tissue compatibility of Spinor.

2.3. Spinor-derived exosomes possessed optimized properties both in quantity and quality

It has been known that stem-cell-derived exosomes play crucial roles for the therapeutic efficacy of MSCs [27,31], which compelled us to investigate the quantity and quality of the Spinor-derived exosomes. Towards this end, exosomes from Spinor and DPMSC were comparatively characterized by transmission electron microscopy (TEM, Fig. S4A), nanoparticle tracking analysis (NTA, Fig. S4B) and the identified markers of exosomes (Fig. S4C). To quantify the amount of exosome, we continuously determinated the total protein content by ELISA in exosomes derived from 1 million cells both in the form of DPMSC and Spinor. As shown in Fig. 2A, Spinor released more amounts of exosomes than DPMSC. For further verification, green fluorescent protein (GFP)-fused CD63 (exosome marker) was stably transfected into the DPMSCs and Spinor, by which the exosomes can be traced by confocal laser scanning microscopy (CLSM) and quantified by fluorescence microplate reader. As shown in Fig. 2B, images of exosomes released from MSC or Spinor were taken by CLSM in which cytoskeleton (FAK) and cell nucleus (DAPI) were dyed in red and blue, respectively. The expression quantity of FAK and the marked cytoskeleton were almost the same both in MSC and Spinor, while much more green exosomes can be found in Spinor (Fig. 2B), which was further supported by the quantitative data of CD63 (Fig. 2C).

The increased amounts of exosomes releasing from Spinor compelled us explore its contents. Thus, we investigated the inclusion protein in Spinor-derived exosome and DPMSC-derived exosome *via* proteome analysis by mass spectrometry. By this way, 643 proteins can be found in the two exosomes as shown in Fig. 2D and 77 of which were differential when comparing Spinor-derived exosome to MSC-derived exosome (adjusted p value < 0.05 and Log2 of fold change >1.3 or < -1.3). Among these differential proteins, 17 (22.0%) proteins were involved in the process in inflammation, 30 (39.0%) proteins were functional for promoting nerve regeneration, 15 (19.5%) proteins were corresponded to scar inhibition and the rest of the proteins (15, 19.5%) were directly related to cell assembly (Fig. 2E), in line with the Kyoto Encyclopedia of Genes and Genomes (KEGG) analysis (Fig. 2F&G). Moreover, gene set enrichment analysis (GSEA) exposed an enrichment of cell-assembly-related protein difference signatures in a consistent and reproducible manner (Fig. S4D), inductive again of the DPMSC assembly and junction in the Spinor. More importantly, the up-regulated pathways of nerve regulation in Spinor-derived exosome comparing with MSC-derived exosome suggested the enhanced ability of spinal cord reparation of Spinor (Fig. S4E, Fig. 2H and I). In addition, this result was supported again by the consistent expression of neurotropic proteins in the Spinor characterized by CLSM (Fig. S4F). Besides, the top down-regulated pathways in MSC assembly included proteins involved in astrocyte proliferation (Fig. 2J and K) and inflammation (Fig. S4G), both of whose suppressions were in favor of the nerve regeneration after spinal cord injury [46,47]. Collectively, these results related to exosomes fully testified to the optimized Spinor-derived exosomes, both in quantity and quality, as a potential tool to repair the injured spinal cord.

2.4. Spinor was more active than MSC to promote the neuronal regeneration and suppress the astrocytes proliferation

To explore the bioaction of Spinor exosomes, the same number of exosomes derived from Spinor and DPMSC were used to incubate with murine primary neuronal cells for three days. In the issue, Spinor-derived exosomes were significantly more active than MSC-derived exosomes and potently promote the regeneration and differentiation of neurons (Fig. 3A). In details, Spinor-derived exosomes resulted in the over threefold increase of branch points (Fig. 3B) and neurite points (Fig. 3C) in sharp contrast to the less than twofold increment by MSC-derived exosomes. Moreover, the additional length of max (Fig. 3D) and mean (Fig. 3E) branch also showed the same tendency. These results demonstrated that Spinor-derived exosomes can potent promote the elongation and differentiation of neurons in more action than MSC-derived exosomes. Of note, both Spinor- and DPMSC-derived exosomes were capable of internalizing into nerve cell (Fig. S5). These results not only suggested that Spinor exosomes should be more active than MSC to promote the neuroplasticity after SCI, but demonstrated the adequate viability of exosomes derived from Spinor.

As our design, Spinor can be an exosome mothership for promoting the neuroplasticity in injured parts after SCI. To verify it *in vivo*, we made 2-mm transverse incisions in rats to establish a model of complete SCI model by cutting the dorsal funiculus spinal cord and dorsal horns at T9-T10 (Fig. S6A). Following the molding, DPMSCs mixing with Matrigel were packed into the cavity at lesion, and Spinor was curled and dressed the wound of spinal cord. One weeks after implantation, histological difference between Spinor or DPMSC implantation were assessed by immunofluorescent staining for exosome (CD63-GFP), neurons (NF) and astrocytes (GFAP). Overlaying with the green fluorescence from the CD63-GFP-labeled exosomes, the red fluorescence signal of neurons was presented in lesion and rostral as well as caudal stumps (Fig. 3F&S6B). Meanwhile, the lessened number of astrocytes after Spinor implantation was obvious in comparation to the GFAP-marked astrocytes in DPMSC-treated rat (Fig. 3G&S6C). Semiquantitative analysis results in Fig. 3H illustrated both amounts and diffusion areas of Spinor-derived exosomes were statistically significantly superior to DPMSC-treated exosomes, suggesting the enhanced viability of exosomes derived from Spinor. Besides, the amounts of neuron in Spinor-treated rats were statistically significantly more than these in DPMSC-treated ones (Fig. 3I), whereas amounts of astrocytes in Spinor-treated rat were statistically significantly less than these in DPMSC-treated rats (Fig. 3J). As it were, these results provide *in vivo* evidence to prove that Spinor was more active than MSC to promote the neuronal regeneration and suppress the astrocytes proliferation.

Additionally, an inflammatory marker, iNOS, was investigated in lesion and rostral as well as caudal stumps to explore the anti-inflammatory ability of Spinor. As shown in Fig. S7A&S7B, significantly decreased inflammation was presented at week 1 after Spinor treatment comparing to the mock and DPMSC treatment, and this result was supported again by the decreased inflammation-induced cell apoptosis measured by Terminal-deoxynucleoitidyl Transferase Mediated Nick End Labeling (TUNEL) staining (Fig. S7C). These results were in good agreement with the proteome analysis that the Spinor-derived exosomes included more anti-inflammatory and less pro-inflammatory proteins (Figs. S4F–G).

2.5. Spinor was more active than MSC to recover the motor and sensory in complete SCI rats

To assess the neuro-regenerative potential of Spinor, 18 rats with complete SCI were divided into three groups: 1) PBS treatment (Ctrl), 2) Spinor treatment and 3) DPMSC treatment, and 6 healthy rats subjected to mock surgery that just included myelotomy and suture without spinal cord transaction were used as positive control. Since immediate treatment after SCI is clinically impossible, all treatments were initiated at

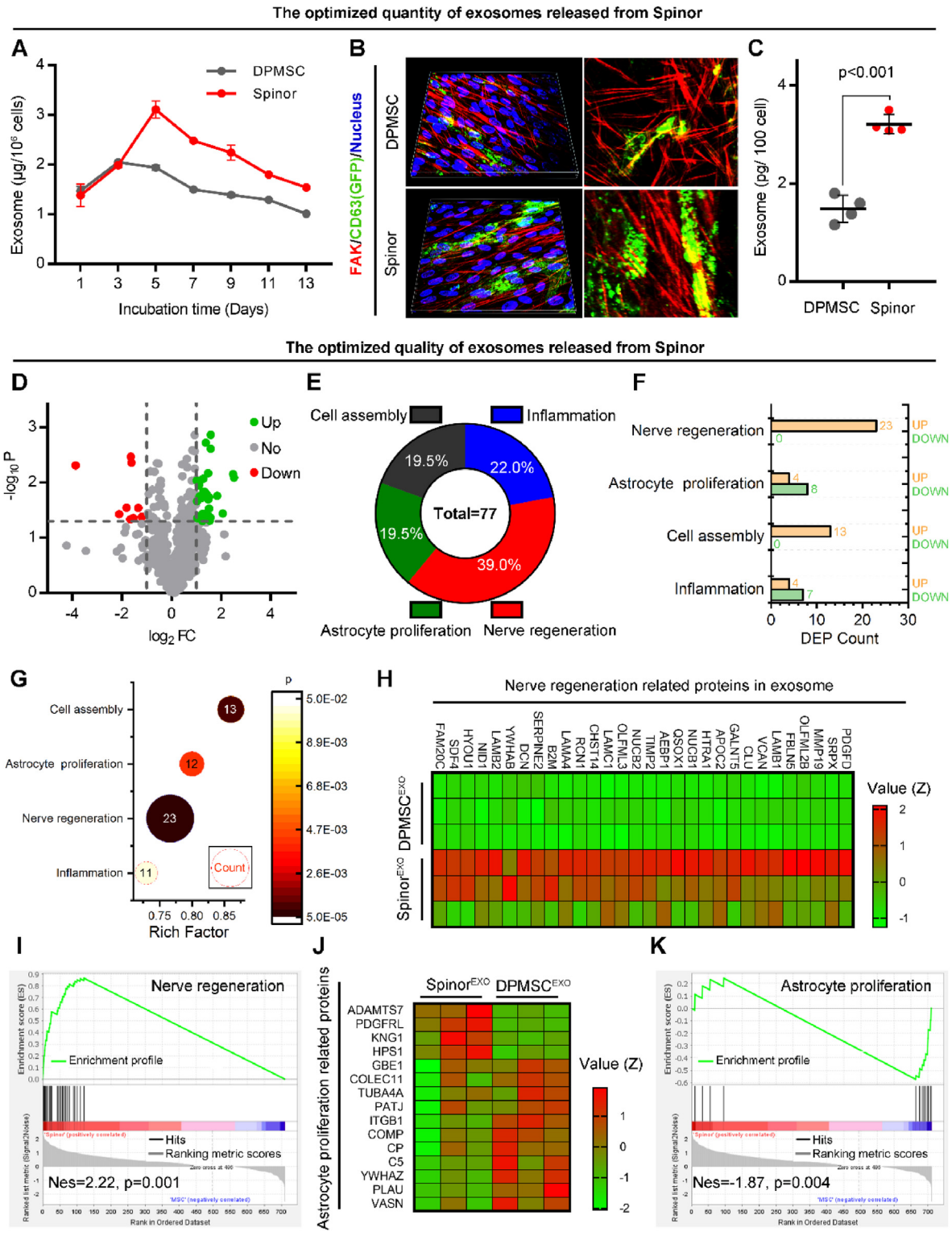

Fig. 2. Spinor-derived exosomes possessed optimized properties both in quantity and quality. (A) The release curve of exosomes from DPMSC and Spinor supernatant within 13 days. The data was presented as the means ± s.d. (n = 3/group). *p* values were calculated by *t*-test. ***$p < 0.001$. (B) Exosome images in MSC and Spinor taken by confocal laser scanning microscopy. Exosomes were labeled by (GFP)-fused CD63, and cytoskeleton as well as cell nucleus were dyed in red (FAK) and blue (DAPI), respectively. Fluorescent intensity results shown as 3D views of surface remodeling presented as angled views (400X). (C) Cumulative release number of exosomes from MSC and Spinor supernatant within 48 h. (D) Volcano plot highlighting significant altered proteins in the comparation between MSX-derived exosomes and Spinor-derived exosomes. (E) The function distribution of differential proteins in D. (F) Bar diagram of KEGG enrichment of differential proteins. (G) KEGG enrichment bubble diagram. (H&I) Gene (Protein) Set Enrichment Analysis (GSEA) (H) and cluster analysis heat map (I) results for the nerve regeneration. (J&K) GSEA (J) and cluster analysis heat map (K) results for the nerve regeneration. (For interpretation of the references to colour in this figure legend, the reader is referred to the Web version of this article.)

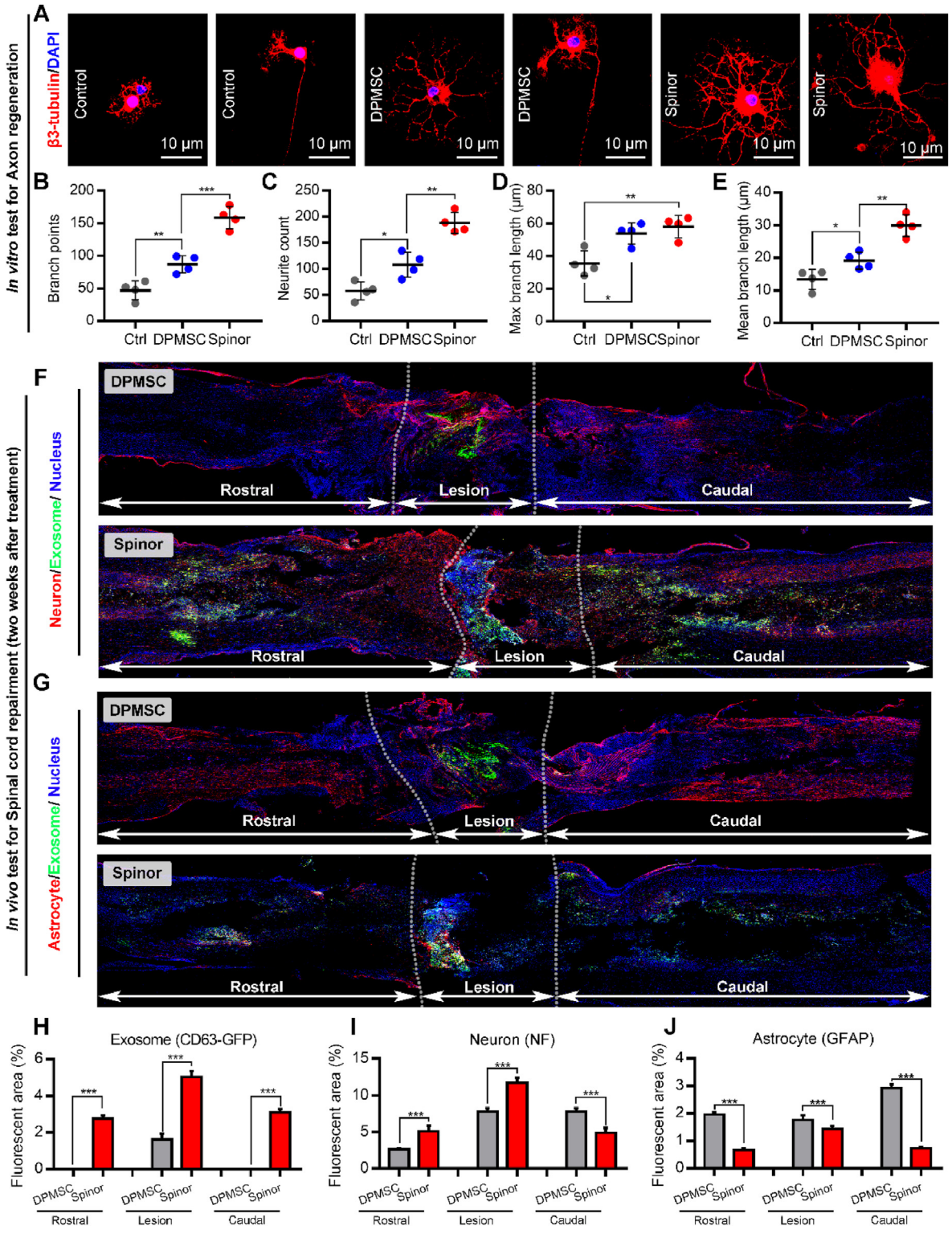

Fig. 3. Spinor was more active than MSC to promote the neuronal regeneration and suppress the astrocytes proliferation. (A) Representative immunofluorescent staining images of spinal cord neurons treated with medium, MSC-Exo, or Spinor-Exo. Neurons marked in red and nuclei marked in blue. Scale bar: 40 μm. (B–E) Branch points (B), neurites count (C), maximum branch level (D) and mean branch length (E), respectively, were measured and compared in all groups. (F) Representative fluorescent micrographs of exosome (GFP-fused CD63 labeled, green) biodistribution and neuron (NF, red) in the host spinal cord tissue. (G) Representative fluorescent micrographs of exosome (green) and astrocyte (GFAP, red) in the host spinal cord tissue. (H–J) The quantized data of the amount of exosome (H), neuron (I) in (F) and astrocyte (J) in (G). The data were presented as the means ± s.d. (n = 3). p values were calculated by ANOVA. *$p < 0.05$, **$p < 0.01$, ***$p < 0.001$. (For interpretation of the references to colour in this figure legend, the reader is referred to the Web version of this article.)

about 3 h postinjury to simulate the actual treatment in clinical case. Following treatments, all rats were subjected to weekly Basso, Beattie and Bresnahan (BBB) locomotor rating scale (Fig. 4A) and weight measurement (Fig. S8A) during an 8-week convalescence. From week 3, rats in Spinor showed significant locomotor recovery (Fig. 4A) accompanying by the lost weight back on (Fig. S8A). At week 8, the average BBB locomotor score of rats in the Spinor group reached 10 ± 2 in sharp contrasts to the mean 2 ± 1 in both mock- and DPMSC- treated rats ($p < 0.001$, Fig. 4A), while Spinor-treated rats gained weight to a greater extent than the other-treated rats (Fig. S8A). Meanwhile, with measuring the electric potential difference from motor cortex to the sciatic nerve of rats, high-amplitude motor-evoked potentials (MEP) can be found in Spinor-treated and healthy groups in sharp contrast to the baseline noise signals measured in mock- and MSC- treated groups (Fig. 4B). As a result, the Spinor treatment resulted in the significant locomotor recovery at 8 weeks posttreatment, whereas neither mock-treated nor MSC-treated rats

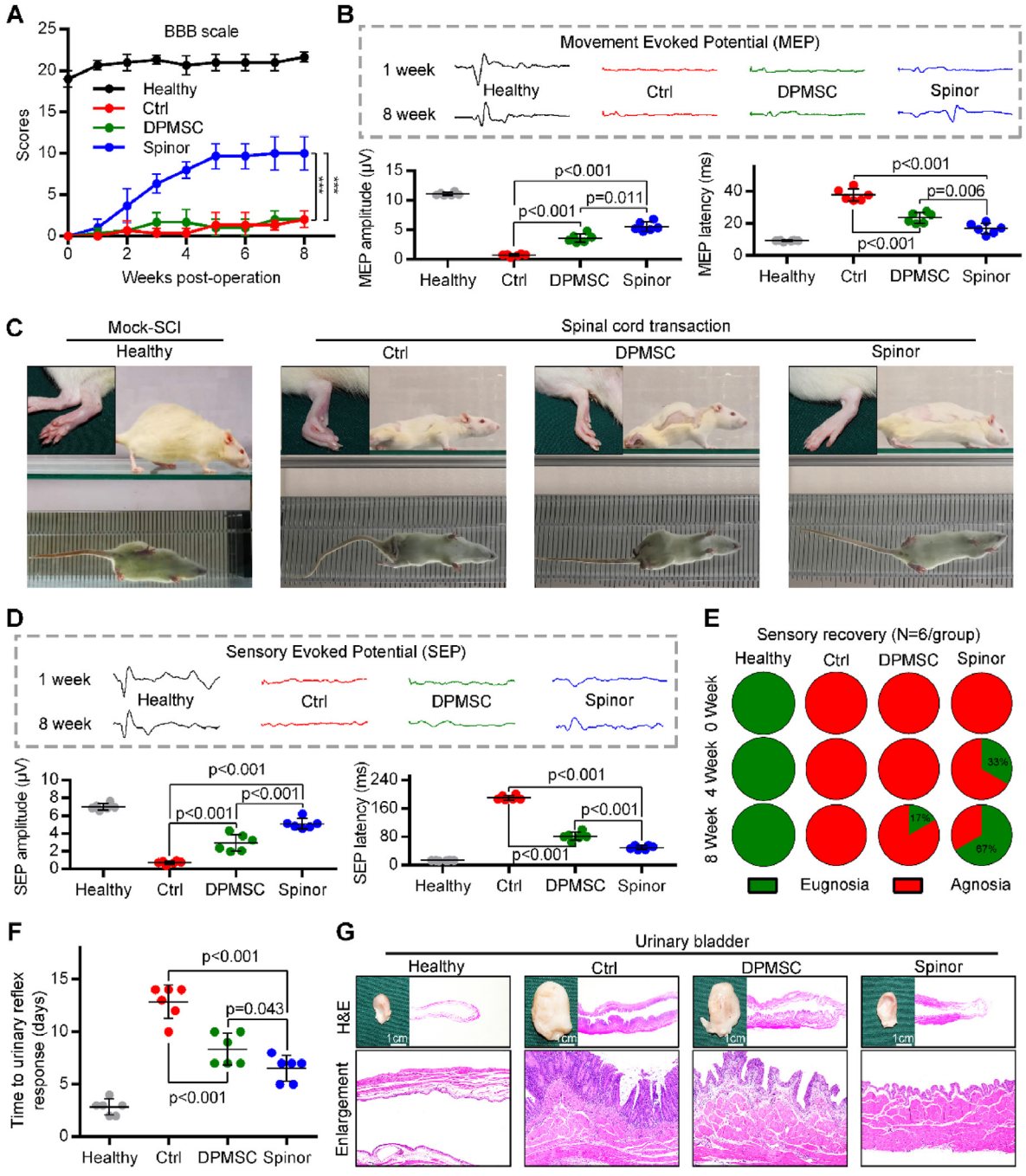

Fig. 4. Spinor was more active than MSC to recover the motor and sensory in complete SCI rats. A) Weekly BBB scores of health rats (Healthy) and complete SCI rats upon PBS (Ctrl), MSC, or Spinor treatment. B) Representative and quantitative movement evoked potentials measured in the healthy rats (black) and mock-treated (red), MSC-treated (green) or Spinor-treated (blue) rats with complete SCI. C) Representative crawling photos of rats in the indicated group at week 8 post-treatment. D) Representative and quantitative sensory evoked potentials measured in the healthy rats (black) and mock-treated (red), MSC-treated (green) or Spinor-treated (blue) rats with complete SCI. E) The Percentage of sensory restorative rats at weeks 0, 4, and 8 post-treatment. F) Bladder function reflected as time to achieve spontaneous urinaryreflex (days) from initiation of treatment. G) Representative photos and H&E staining of bladders from rats in the indicated group at week 8 posttreatment. The data were presented as the means ± s.d. (n = 6/group) *p* values were calculated by ANOVA. *$p < 0.05$, ***$p < 0.001$. (For interpretation of the references to colour in this figure legend, the reader is referred to the Web version of this article.)

can use their hind legs to crawl and even straight back foots (Fig. 4C).

The recovery of athletic ability is always accompanied by the sensory restoration. To verify it, somatosensory evoked potentials (SEP) were recorded at supramaximal stimulation intensities from the coronal screw referenced to the posterior screw in response to the electrical stimulation at the left hind paw of rats. As expected, a characteristic appearance of SEP signal that consisted of three consecutive peaks (two negative and one positive deflections) were observed in healthy and Spinor-treated rats, whereas low amplitude or imperfect signals were measured in the DPMSC- or mock-treated groups (Fig. 4D). To further investigate the sensory recovery, Von Frey filament tests were performed with a gradient of bending forces applying on the hindlimbs ranging from 60 g to 300 g to determine the paw withdrawal threshold. As shown in Fig. 4E, none of the rats in Ctrl group responded to a 300 g filament hair at week 0, 4 and 8, indicative of the complete sensory deficits. Importantly, two-thirds rats in the Spinor-treated group attained sensory recovery at week 8 in sharp

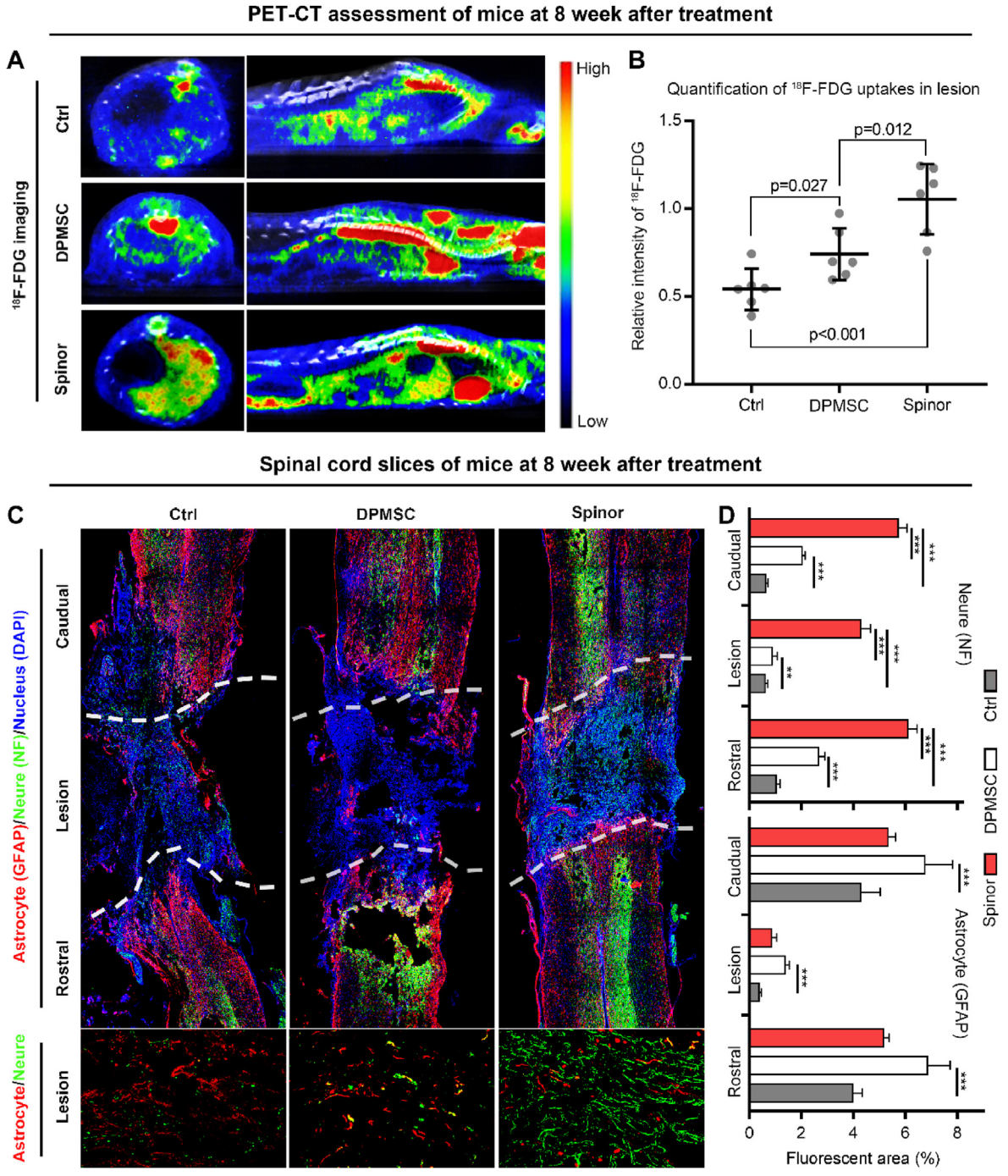

Fig. 5. The histological and cellular mechanisms underlying locomotor and sensory recovery. A) Fusion of Micro-PET images with CT images recorded in the same session and drawing of 3D regions of interest (ROIs) corresponding to each vertebra. B) To quantify glycolysis, relative intensity of [^{18}F]FDG signal was quantified and normalized the sum of the vertebral ROIs percent injected dose per gram of tissue over the total amount of radioactivity in the whole body of the rat, excluding the amount trapped in the tail. C) Representative images showing neurofilaments (NFs, green) and glial fibrillary acidic protein (GFAP, red) staining in Ctrl, MSC and Spinor groups. The white dashed lines in the full views indicated the rostral, lesion, and caudal regions. D) Quantification and comparison of neuron and astrocyte in the two groups. n = 6 per groups. The data were presented as the means ± s.d. of each experiment performed in triplicate. p values were calculated by ANOVA. *$p <$ 0.05, ***$p <$ 0.001. (For interpretation of the references to colour in this figure legend, the reader is referred to the Web version of this article.)

contrast to the only rat in the DPMSC-treated groups (Fig. 4E). In addition, the regain consciousness of urination further support the above results. In details, Spinor-treated rats regained urinary reflex responses in just 6.8 ± 1.6 days, while DPMSC- and mock-treated rats experienced more times without urinary reflex (Fig. 4F), and these results was supported again by the normal-sized bladder (Fig. 4G&S8B) and kidney (Fig. S8C) in Spinor-treated rats. Taken together, these results provide an abundance of evidence that Spinor treatment can recover the sensory in more action than MSC treatment.

2.6. The histological and cellular mechanisms underlying locomotor and sensory recovery

To explore histological mechanisms underlying locomotor and sensory recovery, spinal cord lesions in mock-, Spinor- and DPMSC-treated rats were inspected by a dual-modality imaging combined positron emission tomography (PET) and computed tomography (CT). As for PET imaging, a glucose analog termed 2-[^{18}F]fluoro-2-deoxy-D-glucose ([^{18}F]FDG) was used for measuring the extraction of glucose in spinal cord lesions [48]. Of note, [^{18}F]FDG can uptake into cells with vigorous glucose metabolism, but cannot be decomposed and utilized, thereby accumulating insides these cells [49]. By the merger of [^{18}F] FDG PET and CT imaging as shown in Fig. 5A, a clear sign of [^{18}F]FDG can be found in the lesion of Spinor-treated rat in contrast to the hardly any PET signal in the others. Furthermore, the quantized data of [^{18}F]FDG accumulation in spinal cord lesions support again this result, in which the relative intensity of [^{18}F]FDG in the Spinor-treated lesion statistically significantly exceeded these in others (Fig. 5B).

To identify cellular mechanisms of the SCI therapy, spinal cord lesions and rostral as well as caudal stumps were stained for GFAP, NF, MBP and CGRP to detect astrogliosis, axonal regeneration, Schwann cell regeneration and neurological function, respectively. At week 8 posttreatment, the astrogliosis marker, GFAP expression was significantly up-regulated in DPMSC-treated spinal cord compared with mock-treated ones, while it was barely detectable in the Spinor-treated spinal cord (Fig. 5C, D and Fig. S9A). Moreover, the opposite result can be found in the staining of the neuron marker, NF, in which Spinor treatment caused the most axonal regeneration among the three treatments (Fig. 5C, D and Fig. S9A). In line with it, the up-regulated MBP in Spinor-treated spinal cord illustrated the regeneration of oligodendrocyte, which contributed to the remyelination from regenerative axon to favor functional recovery of spinal cord nervous system (Fig. S9B). Additionally, the increased CGRP level in Spinor-treated spinal cord in comparation to the MSC-treated one supported again that Spinor was more active than MSC to recover the neurological function of spinal cord (Fig. S9B). Taken together, Spinor augmented the regenerative effect through suppressing cicatrization and promoting robust axonal regeneration in the spinal cord lesion.

2.7. Spinor maintained a favorable safety profile

As our design, Spinor can be degraded and absorbed *in vivo*. To test it, Spinor was subcutaneous implantation in healthy rats, and the complete degradation absorption can be found at week 8 after implantation (Fig. S10). To further explore the potential of Spinor for clinical application, we systematically tested the toxicity after subcutaneous transplantation of Spinor. As expected, none immunotoxicity of Spinor were found as evidence by HE staining as well as immunofluorescent staining for immune cell marker (Fig. S11A), Serum inflammatory factor (Fig. S11B) and blood cell count (Fig. S11C and Table S1). Moreover, Histopathological section of heart, liver, spleen, lung and kidney also supported the above findings that Spinor is sufficiently safe as a body filling material (Fig. S11D).

3. Conclusion

This work firstly proved the optimal auxo-action of DPMSC exosome in promoting the regeneration and differentiation of neurons, and a developmentally engineered strategy was established to assemble DPMSCs into a bio-assembly through a three-level sequential induction programme including reductant, energy and mechanical force stimulation. As a spinal cord fascia and exosome mothership, Spinor is in possession of the similar geometric construction and mechanical property with spinal cord and have the optimized capability of exosome secretion in comparation to MSC. More importantly, Spinor exerted multiple mechanisms to create a favorable microenvironment for spinal cord regeneration through inherent and optimized exosome contents involving in suppressing cicatrization as well as inflammation and promoting axonal regeneration. As a result, this *in-situ* treatment by Spinor caused the significant motor improvement, sensory recovery, and faster urinary reflex restoration in complete SCI rats. Collectively, Spinor will provide a promising clinical therapeutic application for severe or even complete SCI after the systematic safety evaluation and pharmacological testing, and supported a new thought to amplify the intrinsic capabilities of stem-cells-derived exosome. More importantly, the developmentally engineered strategy established here will likely have a broad impact on the development of tissue-engineered advanced therapy medicinal products and reinvigorate the efforts for employing stem cells as well as their ramifications in the repair of complex tissues including nervous system.

Credit author statement

Jin Yan: Conceptualization, Methodology, Software, Liqiang Zhang: Data curation, Investigation, Liya Li: Visualization, Investigation. Wangxiao He: Supervision, Writing- Original draft preparation, Writing-Reviewing and Editing. Wenjia Liu: Supervision, Project administration, Funding acquisition.

Declaration of competing interest

The authors declare that they have no known competing financial interests or personal relationships that could have appeared to influence the work reported in this paper.

Acknowledgements

This work was supported by National Natural Science Foundation of China (No. 81970915 for W. Liu), Thousand Talents Plan of Shaanxi Province (For W. He), Natural Science Fund of Shaanxi for distinguished Young Scholars (2020JC33), Natural Science Basic Research Plan in Shaanxi Province of China (No. 2020JQ-092) and Key R & D program of Shaanxi Province (No. 2019KW-074 and No. 2021SF-033) "The Young Talent Support Plan" of Xi'an Jiaotong University (For W. Liu and W. He). We thank Instrument Analysis Center of Xi'an Jiaotong University for their assistance with AFM and SEM analysis. We also appreciate the help of proteomic analysis from BioNovoGene (Suzhou) Co., Ltd.

Appendix A. Supplementary data

Supplementary data to this article can be found online at https://doi.org/10.1016/j.mtbio.2022.100406.

References

[1] G. Nilsson Hall, L.F. Mendes, C. Gklava, L. Geris, F.P. Luyten, I. Papantoniou, Developmentally engineered callus organoid bioassemblies exhibit predictive in vivo long bone healing, Adv. Sci. 7 (2) (2020), 1902295.

[2] E. Seoane Vazquez, V. Shukla, R. Rodriguez-Monguio, Innovation and competition in advanced therapy medicinal products, EMBO Mol. Med. 11 (3) (2019), e9992.
[3] S. Dimmeler, S. Ding, T.A. Rando, A. Trounson, Translational strategies and challenges in regenerative medicine, Nat. Med. 20 (8) (2014) 814–821.
[4] R.S. Marcucio, L. Qin, E. Alsberg, J.D. Boerckel, Reverse engineering development: crosstalk opportunities between developmental biology and tissue engineering, J. Orthop. Res. 35 (11) (2017) 2356–2368.
[5] T. Takebe, M. Enomura, E. Yoshizawa, M. Kimura, H. Koike, Y. Ueno, T. Matsuzaki, T. Yamazaki, T. Toyohara, K. Osafune, Vascularized and complex organ buds from diverse tissues via mesenchymal cell-driven condensation, Cell Stem Cell 16 (5) (2015) 556–565.
[6] N.C. Rivron, J. Frias-Aldeguer, E.J. Vrij, J.-C. Boisset, J. Korving, J. Vivié, R.K. Truckenmüller, A. Van Oudenaarden, C.A. Van Blitterswijk, N. Geijsen, Blastocyst-like structures generated solely from stem cells, Nature 557 (7703) (2018) 106–111.
[7] C.J. Michael, A.M. Zachary, D.A. Tej, M.D. Vanessa, V. Anand, Stem cell therapies for acute spinal cord injury in humans: a review, Neurosurg. Focus 46 (3) (2019) E10.
[8] R. Kumar, J. Lim, R.A. Mekary, A. Rattani, M.C. Dewan, S.Y. Sharif, E. Osorio-Fonseca, K.B. Park, Traumatic spinal injury: global epidemiology and worldwide volume, World Neurosurg 113 (2018) e345–e363.
[9] T.H. Hutson, S. Di Giovanni, The translational landscape in spinal cord injury: focus on neuroplasticity and regeneration, Nat. Rev. Neurol. 15 (12) (2019) 732–745.
[10] V. Veneruso, F. Rossi, A. Villella, A. Bena, G. Forloni, P. Veglianese, Stem cell paracrine effect and delivery strategies for spinal cord injury regeneration, J. Contr. Release 300 (2019) 141–153.
[11] G. García-Alías, S. Barkhuysen, M. Buckle, J.W. Fawcett, Chondroitinase ABC treatment opens a window of opportunity for task-specific rehabilitation, Nat. Neurosci. 12 (9) (2009) 1145–1151.
[12] J. McCall, N. Weidner, A. Blesch, Neurotrophic factors in combinatorial approaches for spinal cord regeneration, Cell Tissue Res. 349 (1) (2012) 27–37.
[13] R.R. Williams, M. Henao, D.D. Pearse, M.B. Bunge, Permissive Schwann cell graft/spinal cord interfaces for axon regeneration, Cell Transplant. 24 (1) (2015) 115–131.
[14] V. Sahni, J.A. Kessler, Stem cell therapies for spinal cord injury, Nat. Rev. Neurol. 6 (7) (2010) 363–372.
[15] S. Guo, N. Perets, O. Betzer, S. Ben-Shaul, A. Sheinin, I. Michaelevski, R. Popovtzer, D. Offen, S. Levenberg, Intranasal delivery of mesenchymal stem cell derived exosomes loaded with phosphatase and tensin homolog siRNA repairs complete spinal cord injury, ACS Nano 13 (9) (2019) 10015–10028.
[16] P. Lu, Y. Wang, L. Graham, K. McHale, M. Gao, D. Wu, J. Brock, A. Blesch, Ephron S. Rosenzweig, Leif A. Havton, B. Zheng, James M. Conner, M. Marsala, Mark H. Tuszynski, Long-distance growth and connectivity of neural stem cells after severe spinal cord injury, Cell 150 (6) (2012) 1264–1273.
[17] H. Sabelström, M. Stenudd, P. Réu, D.O. Dias, M. Elfineh, S. Zdunek, P. Damberg, C. Göritz, J. Frisén, Resident neural stem cells restrict tissue damage and neuronal loss after spinal cord injury in mice, Science 342 (6158) (2013) 637.
[18] Y. Qian, H. Lin, Z. Yan, J. Shi, C. Fan, Functional nanomaterials in peripheral nerve regeneration: scaffold design, chemical principles and microenvironmental remodeling, Mater. Today 51 (2021) 165–187.
[19] H. Jiang, Y. Qian, C. Fan, Y. Ouyang, Polymeric guide conduits for peripheral nerve tissue engineering, Front. Bioeng. Biotechnol. 8 (2020).
[20] J. Yan, R. Wu, S. Liao, M. Jiang, Y. Qian, Applications of polydopamine-modified scaffolds in the peripheral nerve tissue engineering, Front. Bioeng. Biotechnol. 8 (2020).
[21] Y. Qian, X. Wang, J. Song, W. Chen, S. Chen, Y. Jin, Y. Ouyang, W.-E. Yuan, C. Fan, Preclinical assessment on neuronal regeneration in the injury-related microenvironment of graphene-based scaffolds, NPJ Regenerat. Med. 6 (1) (2021) 31.
[22] L. Zhan, J. Deng, Q. Ke, X. Li, Y. Ouyang, C. Huang, X. Liu, Y. Qian, Grooved fibers: preparation principles through electrospinning and potential applications, Adv. Fiber Mater. 4 (2) (2022) 203–213.
[23] E. Curtis, J.R. Martin, B. Gabel, N. Sidhu, T.K. Rzesiewicz, R. Mandeville, S. Van Gorp, M. Leerink, T. Tadokoro, S. Marsala, C. Jamieson, M. Marsala, J.D. Ciacci, A first-in-human, phase I study of neural stem cell transplantation for chronic spinal cord injury, Cell Stem Cell 22 (6) (2018) 941–950, e6.
[24] J.-H. Huang, X.-M. Yin, Y. Xu, C.-C. Xu, X. Lin, F.-B. Ye, Y. Cao, F.-Y. Lin, Systemic administration of exosomes released from mesenchymal stromal cells attenuates apoptosis, inflammation, and promotes angiogenesis after spinal cord injury in rats, J. Neurotrauma 34 (24) (2017) 3388–3396.
[25] Z. Zhou, Y. Chen, H. Zhang, S. Min, B. Yu, B. He, A. Jin, Comparison of mesenchymal stromal cells from human bone marrow and adipose tissue for the treatment of spinal cord injury, Cytotherapy 15 (4) (2013) 434–448.
[26] I. Vismara, S. Papa, F. Rossi, G. Forloni, P. Veglianese, Current options for cell therapy in spinal cord injury, Trends Mol. Med. 23 (9) (2017) 831–849.
[27] M.Z. Ratajczak, T. Jadczyk, D. Pędziwiatr, W. Wojakowski, New advances in stem cell research: practical implications for regenerative medicine, Pol. Arch. Med. Wewn. 124 (7) (2014) 417–426.
[28] M.V. Sofroniew, Dissecting spinal cord regeneration, Nature 557 (7705) (2018) 343–350.
[29] J.E. Burda, M.V. Sofroniew, Reactive gliosis and the multicellular response to CNS damage and disease, Neuron 81 (2) (2014) 229–248.
[30] M.V. Sofroniew, Astrocyte barriers to neurotoxic inflammation, Nat. Rev. Neurosci. 16 (5) (2015) 249–263.
[31] C. Théry, L. Zitvogel, S. Amigorena, Exosomes: composition, biogenesis and function, Nat. Rev. Immunol. 2 (8) (2002) 569–579.
[32] A. Marote, F.G. Teixeira, B. Mendes-Pinheiro, A.J. Salgado, MSCs-derived exosomes: cell-secreted nanovesicles with regenerative potential, Front. Pharmacol. 7 (2016) 231.
[33] L. Li, Y. Zhang, J. Mu, J. Chen, C. Zhang, H. Cao, J. Gao, Transplantation of human mesenchymal stem-cell-derived exosomes immobilized in an adhesive hydrogel for effective treatment of spinal cord injury, Nano Lett. 20 (6) (2020) 4298–4305.
[34] N. Perets, O. Betzer, R. Shapira, S. Brenstein, A. Angel, T. Sadan, U. Ashery, R. Popovtzer, D. Offen, Golden exosomes selectively target brain pathologies in neurodegenerative and neurodevelopmental disorders, Nano Lett. 19 (6) (2019) 3422–3431.
[35] Y.H. Chang, K.C. Wu, H.J. Harn, S.Z. Lin, D.C. Ding, Exosomes and stem cells in degenerative disease diagnosis and therapy, Cell Transplant. 27 (3) (2018) 349–363.
[36] K.T. Wright, W.E. Masri, A. Osman, J. Chowdhury, W.E.B. Johnson, Concise review: bone marrow for the treatment of spinal cord injury: mechanisms and clinical applications, Stem Cell. 29 (2) (2011) 169–178.
[37] M.C. Jin, Z.A. Medress, T.D. Azad, V.M. Doulames, A. Veeravagu, Stem cell therapies for acute spinal cord injury in humans: a review, Neurosurg. Focus 46 (3) (2019) E10.
[38] S.J. Butler, M.E. Bronner, From classical to current: analyzing peripheral nervous system and spinal cord lineage and fate, Dev. Biol. 398 (2) (2015) 135–146.
[39] R. Massarwa, H.J. Ray, L. Niswander, Morphogenetic movements in the neural plate and neural tube: mouse, Wiley Interdiscip. Rev. Dev. Biol. 3 (1) (2014) 59–68.
[40] F. Wei, C. Qu, T. Song, G. Ding, Z. Fan, D. Liu, Y. Liu, C. Zhang, S. Shi, S. Wang, Vitamin C treatment promotes mesenchymal stem cell sheet formation and tissue regeneration by elevating telomerase activity, J. Cell. Physiol. 227 (9) (2012) 3216–3224.
[41] Y. Wu, D.S. Puperi, K.J. Grande-Allen, J.L. West, Ascorbic acid promotes extracellular matrix deposition while preserving valve interstitial cell quiescence within 3D hydrogel scaffolds, J. Tissue Eng. Regen. Med. 11 (7) (2017) 1963–1973.
[42] J.W. Locasale, L.C. Cantley, Metabolic flux and the regulation of mammalian cell growth, Cell Metabol. 14 (4) (2011) 443–451.
[43] Y.n. Hu, F. Zhang, W. Zhong, Y.n. Liu, Q. He, M. Yang, H. Chen, X. Xu, K. Bian, J. Xu, J. Li, Y. Shen, H. Zhang, Transplantation of neural scaffolds consisting of dermal fibroblast-reprogrammed neurons and 3D silk fibrous materials promotes the repair of spinal cord injury, J. Mater. Chem. B 7 (47) (2019) 7525–7539.
[44] T. Yu, L. Wen, J. He, Y. Xu, T. Li, W. Wang, Y. Ma, M.A. Ahmad, X. Tian, J. Fan, X. Wang, H. Hagiwara, Q. Ao, Fabrication and evaluation of an optimized acellular nerve allograft with multiple axial channels, Acta Biomater. 115 (2020) 235–249.
[45] I. Matai, G. Kaur, A. Seyedsalehi, A. McClinton, C.T. Laurencin, Progress in 3D bioprinting technology for tissue/organ regenerative engineering, Biomaterials 226 (2020), 119536.
[46] T.M. O'Shea, J.E. Burda, M.V. Sofroniew, Cell biology of spinal cord injury and repair, J. Clin. Invest. 127 (9) (2017) 3259–3270.
[47] M.B. Orr, J.C. Gensel, Spinal cord injury scarring and inflammation: therapies targeting glial and inflammatory responses, Neurotherapeutics 15 (3) (2018) 541–553.
[48] C.G. Radu, C.J. Shu, S.M. Shelly, M.E. Phelps, O.N. Witte, Positron emission tomography with computed tomography imaging of neuroinflammation in experimental autoimmune encephalomyelitis, Proc. Natl. Acad. Sci. U.S.A. 104 (6) (2007) 1937–1942.
[49] J. Czernin, W.A. Weber, H.R. Herschman, Molecular imaging in the development of cancer therapeutics, Annu. Rev. Med. 57 (1) (2006) 99–118.